Ab initio calculation of excitons in ZnO

Robert Laskowski[1,2] and Niels Egede Christensen[1]
[1]*Department of Physics and Astronomy, University of Århus, DK-8000 Århus C, Denmark*
[2]*Institute of Materials Chemistry, Technische Universität Wien, Getreidemarkt 9/165TC, A-1060 Vienna, Austria*
(Received 2 September 2005; published 5 January 2006)

The optical absorption and excitonic properties of wurtzite ZnO are investigated by means of an *ab initio* approach taking into account electron-hole correlations. This is done by solving the Bethe-Salpeter equation, using the results of density functional theory calculations as a starting point. Our main focus is the calculation of the band edge optical spectra. We have identified ground states for three excitons (*A*, *B*, and *C*), with binding energies around 68 meV. Excitons *A* and *B* are excited mainly by light polarized perpendicular to the *c* crystallographic axis. The *C* exciton absorbs mainly light polarized parallel to the *c* axis. Due to spin-orbit interactions, excitons *A* and *C* show a tiny absorption for the parallel polarization and perpendicular polarizations, respectively.

DOI: 10.1103/PhysRevB.73.045201 PACS number(s): 71.15.Qe, 71.35.Cc, 78.20.Ci, 78.40.Fy

I. INTRODUCTION

Zinc oxide is a direct band-gap semiconductor crystallizing in the wurtzite structure and exhibiting strong excitonic effects even at temperatures above 300 K. Due to its large band gap (3.4 eV), it is an attractive candidate for applications in visible and ultraviolet light emitters, transparent field-effect transistors, sensors, and piezoelectric devices.[1–3] Since excitons in ZnO are stable even at room temperature, this material is also considered for the realization of a room-temperature polariton laser.[4,5]

Similar to the most binary semiconductors, the lowest conduction-band edge of ZnO is mainly *s* like, whereas the states at the valence-band maximum (VBM) are *p* like. Both edges are located at the Γ point of the Brillouin zone (BZ). At the VBM spin-orbit coupling (SOC) splits the atomic *p* level into two states, one being $(j=3/2)$ fourfold and the other $(j=1/2)$ doubly degenerate. Further, the hexagonal crystal field splits the $j=3/2$ level into two doubly degenerate states. When SOC and spin degrees of freedom are neglected the crystal field splits the threefold-degenerate *p* level into a nondegenerate state and doubly degenerate one in the standard notation denoted as Γ_1 and Γ_5. In the double group notation the Γ_1 state is denoted as Γ_7. SOC splits the nonrelativistic state Γ_5 into Γ_7 and Γ_9, also in double group notation. A detailed description of the relativistic band structures of wurtzite type semiconductors is given in Ref. 6, and a possible energy-level diagram at the VBM is shown in Fig. 1.

The ordering of the bands at the VBM in ZnO has been discussed for a long time. From their early studies of the polarization dependence of reflectivity spectra Thomas[7] and Hopfield[8] concluded that the energetic ordering at the VBM should be Γ_7, Γ_9, Γ_7. This sequence was attributed to a spin-orbit splitting parameter which is negative as a result of hybridization with the Zn *d* states and corresponds to the sketch in Fig. 1. Based on absorption and reflection spectra of four different samples Park *et al.*[9] claimed the Γ_9, Γ_7, Γ_7 ordering, Γ_9 being the state with the highest energy. Later, Reynolds *et al.*,[10] after analysis of polarized reflectance and magnetophotoluminescence, also arrived at the conclusion that the ordering should be Γ_9, Γ_7, Γ_7, and more recent studies of Chichibu *et al.*[11] and Adachi *et al.*[12] further supported this picture. Contrary to this, the recent experiments on the magneto-optical properties of bound excitons[13,14] provide evidence of Γ_7 symmetry of the upper valence band. Moreover, the Γ_9, Γ_7, Γ_7 assignments are questioned in the theoretical work by Lambrecht *et al.*[15] based on density functional theory (DFT), and it is argued that the original sequence proposed by Thomas and Hopfield is correct. The present work agrees with this.

The electronic structure at the VBM in ZnO and, thus, its optical properties near the absorption edge are strongly influenced by hybridization with the Zn 3*d* states. In order to perform reliable Bethe-Salpeter-equation (BSE) calculations it is important that the basic quasiparticle band structure in-

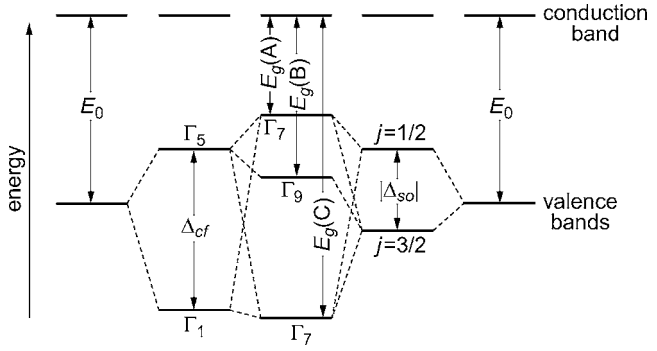

FIG. 1. Schematic energy-level diagram of band splitting under action of the crystal-field and spin-orbit interactions in wurtzite crystals (from Ref. 6, but changed to the case with negative Δ_{SO}). To the left, splitting induced only by the crystal field, to the right splitting induced only by the spin-orbit interaction. The combined case is shown in the middle. The gaps $E_g(A)$, $E_g(B)$, and $E_g(C)$ which enter in the calculations of the binding energies of *A*, *B*, and *C* excitons, respectively, are indicated in the middle. Note that due to spin degeneracy the indicated levels are doubly degenerate. In the picture suggested by Park *et al.* (Ref. 9) and Reynolds *et al.* (Ref. 10) the uppermost Γ_9 and Γ_7 levels are interchanged (and the $j=1/2$ and $j=3/2$ levels to the right are also interchanged).

cludes this effect correctly. It is well known that DFT yields $3d$ states in Zn which are too high[16] in energy and that this affects spectral as well as cohesive properties. Also in ZnO DFT predicts the spectral position of the Zn $3d$ density of states (DOS) incorrectly.[15] In that case the overestimate of the hybridization between the VBM states and the d shell leads to a too large SOC-induced splitting of the Γ_9 and Γ_7. Corrections which lower the energies of semicore states can be made, for example,[16,17] by means of self-consistent self-interaction-corrected (SIC) calculations[18] or simplified SIC calculations. In the present work we have chosen to use the LDA+U method with parameters extrapolated from the values calculated for other d elements[19] and show that this significantly improves the calculated optical spectra.

In this work we solve the Bethe-Salpeter equation for ZnO and calculate the excitonic spectra directly from first principles. The symmetry properties of the excitons in ZnO and as well as for other hexagonal semiconductors can be deduced from the symmetries of the bands involved in the respective transitions, their (reducible) representations being given by the direct products of the irreducible representations of the conduction band (Γ_7) and VBM states (Γ_9 or Γ_7). The decompositions of these products into irreducible representations are

$$\Gamma_7 \times \Gamma_9 \rightarrow \Gamma_5 + \Gamma_6,$$

$$\Gamma_7 \times \Gamma_7 \rightarrow \Gamma_5 + \Gamma_1 + \Gamma_2.$$

The dipole transitions with symmetries Γ_6 and Γ_2 are forbidden. The excitons with symmetries Γ_5 and Γ_1 are dipole active for light polarization perpendicular and parallel, respectively, to the hexagonal c axis. These relations are useful for identification of the excitons in calculated or measured spectra. The exciton associated with the transition between bands, $\Gamma_7 \rightarrow \Gamma_7$, is visible for both perpendicular and parallel polarizations, whereas the excitons associated with the $\Gamma_9 \rightarrow \Gamma_7$ transition is only visible for light polarized perpendicular to the c axis.

The paper is organized as follows. The next section describes the basic ingredients of the computational methods we have applied. Section III presents and discusses the results of our calculations. Finally, Sec. IV concludes and summarizes our findings.

II. COMPUTATIONAL METHOD

The computational scheme for calculating the optical response that takes into account the electron-hole interaction employed in this work has already been introduced and applied by several authors.[20–22] The rigorous theoretical description of the e-h excitations is based on the equation of motion of the two-particle Green's function, known as the Bethe-Salpeter equation. The computational procedure solves this equation in approximate manner represented in the form of an effective eigenvalue problem with the so-called BSE Hamiltonian:[23,24]

$$\sum_{v'c'\mathbf{k}'} H^{e}_{vc\mathbf{k},v'c'\mathbf{k}'} A^{\lambda}_{v'c'\mathbf{k}'} = E^{\lambda} A^{\lambda}_{vc\mathbf{k}}. \tag{1}$$

The equation is formulated in the basis of electron and hole quasiparticle states. The excitation spectrum is given by the eigenvalues of this equation. In this formalism only direct transitions leading to e-h-excited states with infinite lifetime are considered. In Eq. (1), H^e is the effective e-h interaction and $vc\mathbf{k}$ denotes an elementary excitation taking place at a point $\mathbf{k}$ of the Brillouin zone, from a valence (v) to a conduction (c) band. The actual excitonic eigenstate is a linear combination of such elementary excitations. The effective BSE Hamiltonian is thus a sum of three terms:

$$H^{e} = H^{diag} + H^{dir} + H^{x}, \tag{2}$$

which are defined as

$$H^{diag}_{vc\mathbf{k},v'c'\mathbf{k}'} = (\varepsilon_{v\mathbf{k}} - \varepsilon_{c\mathbf{k}} + \Delta)\,\delta_{vv'}\delta_{cc'}\delta_{\mathbf{k}\mathbf{k}'}, \tag{3}$$

$$H^{dir}_{vc\mathbf{k},v'c'\mathbf{k}'} = -\int \mathrm{d}^3r\mathrm{d}^3r'\,\psi_{v\mathbf{k}}(\mathbf{r})\psi^{*}_{c\mathbf{k}}(\mathbf{r}') \times W(\mathbf{r},\mathbf{r}')\psi^{*}_{v'\mathbf{k}'}(\mathbf{r})\psi_{c'\mathbf{k}'}(\mathbf{r}'), \tag{4}$$

$$H^{x}_{vc\mathbf{k},v'c'\mathbf{k}'} = \int \mathrm{d}^3r\mathrm{d}^3r'\,\psi_{v\mathbf{k}}(\mathbf{r})\psi^{*}_{c\mathbf{k}}(\mathbf{r}) \times \bar{v}(\mathbf{r},\mathbf{r}')\psi^{*}_{v'\mathbf{k}'}(\mathbf{r}')\psi_{c'\mathbf{k}'}(\mathbf{r}'). \tag{5}$$

The direct interaction term H^{dir} describes the screened Coulomb attraction (W) between the hole and electron. The necessary dielectric matrix is calculated within the random phase approximation (RPA) including local field effects.[25,26] Note that the exchange part of the Hamiltonian, H^x, involves the short-range part of the bare Coulomb interaction ($\bar{v}$). Neglecting the direct and exchange terms leaves only the diagonal part of the Hamiltonian (H^{diag}) and results in an independent e-h approximation. The quasiparticle states, which are the basis of the BSE Hamiltonian, are often well approximated by the DFT wave functions,[27] but the the conduction-band energies are too close to the VBM. In order to simplify calculations, we construct our Hamiltonian directly using the DFT eigenstates and we approximate the self-energy by an appropriate rigid shift of the conduction bands. This so-called "scissors operator" or "scissors shift" Δ is determined by adjusting the DFT band gap to the measured value.[28] As this shift only appears explicitly in the diagonal part of the Hamiltonian, it has no direct effect on the binding energies. It influences, however, the excitonic eigenenergies indirectly through its effect on the screening interaction (the scissor shifted DFT states are used when calculating the screening within the RPA).

The linearized augmented plane-wave method plus local orbitals (LAPW+LO) is used to calculate single-particle states.[29] We have used the improved form of the basis set, where the linearization is moved from augmented plane waves into additional local orbitals.[30] The implementation of the BSE scheme within LAPW method has already been applied to centrosymmetric[31–33] and noncentrosymmetric[34] sys-

tems. DFT calculations were performed within generalized gradient approximation (GGA), using the Perdew-Burke-Ernzerhof parametrization of the exchange-correlation potential.[35]

It has already been shown[15] that DFT with LDA or GGA places the Zn d peak of the density of states in ZnO much too close to the valence states. This affects the hybridization of the Zn d states with valence bands and results in incorrect spin-orbit and crystal field splitting. In order to correct this deficiency we applied so called LDA+U method.[36] The method allows for a non-LDA and GGA-treatment of selected set of orbitals with an orbital dependent potential defined by Coulomb and exchange parameters U and J. In our case they are d orbitals of the Zn atom. LDA+U can be formulated with several different double-counting corrections (DCC's): namely, the "fully localized limit" (FLL),[37] "around the mean field" (AMF),[38] and the recently proposed DFT-DCC.[39] Because the d shell in Zn is full, the FLL is the only applicable formulation in our case. In this approach the extra potential applied to the d shell is of the form

$$V^{FLL} = (U - J)\left(\frac{1}{2} - \hat{n}_\sigma\right), \tag{6}$$

where n_σ gives the occupancy of the orbital σ. In order to avoid double counting in the nonspherical part of the potential, $U_{eff} = U - J$ is used instead of separate U and J, and also the multipolar term proportional to J in the LDA+U potential is omitted.

III. RESULTS

The excitation energies are calculated by diagonalization of the eigenvalue equation (1), which is formulated in the basis of DFT eigenstates indexed by valence and conduction bands, and **k**-point indices. It turns out that an enormously dense **k**-point sampling is required to reach numerical convergence. This is related to the fact that the excitonic envelope function is very delocalized in real space and, at the same time, localized in **k** space. Closer analysis shows that only excitations between the topmost valence and the lowest conduction bands, around the center of the BZ (Γ point), enter into the wave function of the lowest excitons. This means that, as far as we are interested in the excitation with energies around the band gap, the BSE Hamiltonian can be considered as block diagonal in the **k** index localized around Γ. The outer region does not need to be sampled at all, and the required density of **k** points can be reached. The number of **k** points can be kept low enough that makes the diagonalization of Eq. (1) possible. A similar approach has been used for calculation of the binding energies of excitons in GaAs (Ref. 22) and GaN (Ref. 34). Two parameters control the sampling: i.e., the volume of the sampled region and the number of k points inside. The computational cost is proportional to the number of k points only. In the calculations presented in this work we have used sampling with $13 \times 13 \times 13$ mesh (only points that are consistent with the hexagonal symmetry were kept). In order to reach the desired density several calculations with gradually decreased sampled region have been performed. For large volumes only the Γ point contributes to the excitonic wave functions, resulting in completely delocalized excitons. For the optimal volume the excitonic envelope function should be properly sampled, and at the same time it should be well confined inside the sampled region. We have found that, for the experimental structure parameters ($c/a = 1.602$, $u = 0.382$, and volume), accurate results for ground state are obtained by sampling a $1/9 \times 1/9 \times 1/4$ fraction of the BZ which corresponds to the density equivalent to 7×10^5 points in a full BZ.

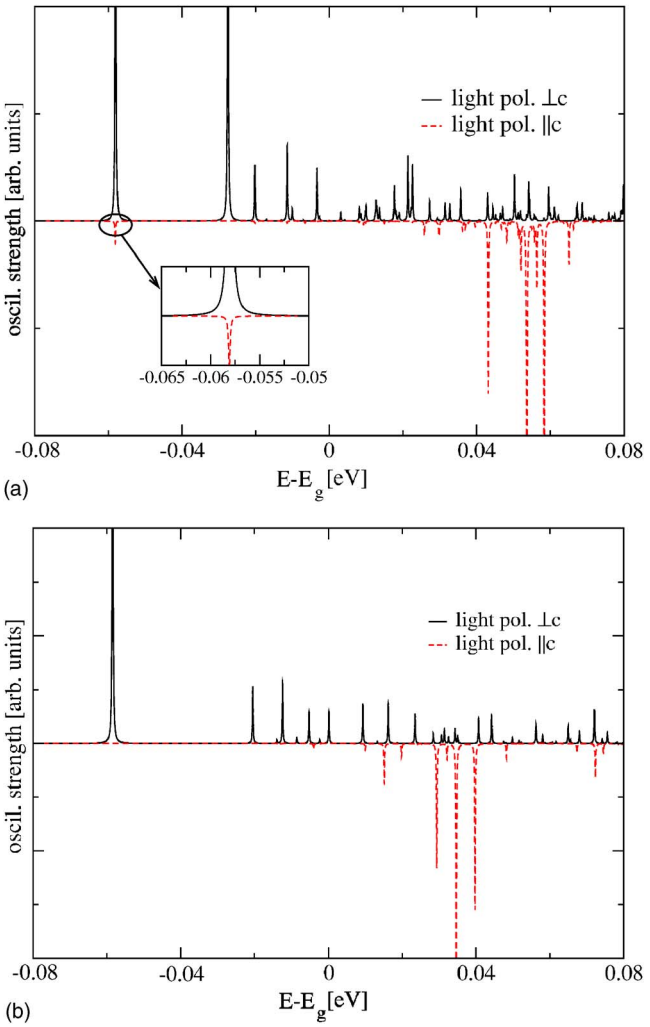

FIG. 2. (Color online) Band-edge absorption in ZnO calculated with the GGA, (a) results with SOC, (b) results without SOC. E_g is the fundamental gap—i.e., $E_g(A)$, where A is the uppermost VBM level.

The calculations of excitonic spectra have been done with and without SOC included into the DFT Hamiltonian. In the SOC case, six valence and two conduction bands have been included in the BSE Hamiltonian. In the non-SOC case spin degrees of freedom can be eliminated and the number is reduced to three valence states and one conduction band. The schematic diagram of these bands at Γ point is presented in Fig. 1. Figure 2 presents band-edge absorption calculated with GGA band structure. For calculations without SOC and light polarized perpendicular to the crystallographic c axis there are four well-separated peaks in the band gap. The first

one appears at about −58 meV. This peak consists of two degenerate excitonic levels. For light polarized parallel to the *c* axis there are no peaks below the conduction band edge. The spectra calculated with SOC show naturally more peaks. We can see that the first peak in non-SOC spectra for perpendicular polarization splits into two peaks, at 58 meV and 28 meV. These peaks are usually referred to as *A* and *B* excitons. Apart from a small signal at the position of the *A* exciton, the peaks for parallel polarization appear only above the conduction-band edge. In comparison to the non-SOC spectra this group of peaks is slightly shifted towards higher photon energies. The small peak at the position of the *A* exciton indicates that the valence band contributing to this exciton is of Γ_7 symmetry. Comparing these results to the measurements we see that the position of the first peak for perpendicular polarization quite well agrees with the experimental binding energies.[40] However, the SOC-induced splitting between *A* and *B* peaks, which is here about 30 meV, is around 15 times larger than the value estimated from experiments (2.4 meV).[41] Further, for the parallel polarization we do not have any peak corresponding to the experimentally observed *C* exciton inside the band gap. These discrepancies are due to errors in the basic GGA band calculation where the Zn 3*d* bands are lying at too high energies, which causes these states to hybridize too strongly with the VBM states.[15] The calculated DOS is presented in Fig. 3. The Zn *d* peak almost touches the valence region of the DOS and spreads between −4 and −6 eV relative to the valence-band edge. According to the photoemission measurements the position should be around −7 eV.[42] The source of this error is related to the insufficient treatment of electron correlations in the Zn *d* shell by the GGA.

It is known that the description of the correlation can be improved by application of an orbital-dependent potential given by the so-called LDA+*U* method.[36–39] The application of this method is complicated by the fact that, in general, the potential is derived on the basis of two empirical parameters *U* and *J*, which, however, have a clear physical interpretation. *U* and *J* are average screened Coulomb and exchange interactions on a given atom in a given shell. Besides, *U* and *J* can be calculated from first principles.[19,43] Solovyev *et al.*[19] have calculated the values of *U* and *J* for series of 3*d* metals, from Ti to Cu, in LaMO_3 compounds. They showed that the parameters scale linearly with the number of electrons in the *d* shell. Extrapolating this linear dependence to the Zn case with ten electrons on the *d* shell we get for *U* a value of about 9 eV and for *J* approximately 1.2 eV. Because we use a spherically symmetric formulation of the LDA+*U*, only an effective $U_{eff}=U-J$ needs to be defined. The density of states resulting from LDA+*U* calculations is presented in Fig. 3. The Zn *d* peak has moved down the energy scale, with its average position now close to −7 eV, which agrees perfectly with photoemission. The downshifted *d* bands are narrower, spanning the region between −6.2 and −7.8 eV. Also, the *d* character in the VBM states has been considerably reduced as compared to the pure GGA calculations. In the previous linear muffin-tin orbital (LMTO) calculations, the position of the *d* levels was optimized with respect to crystal field and spin-orbit splittings and was found to be 6.25 eV below the valence-band maximum.[15] The effects of

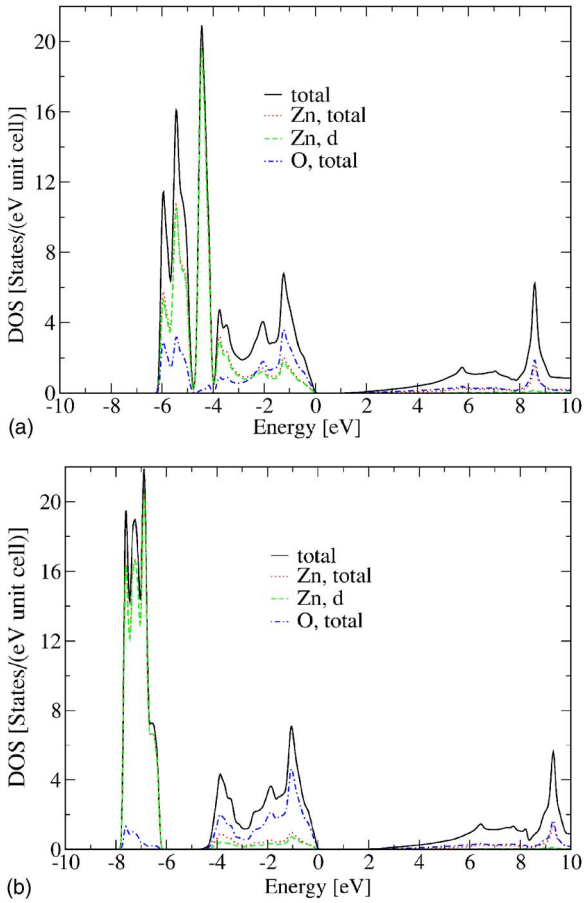

FIG. 3. (Color online) Density of states of ZnO calculated with (a) LDA and (b) with LDA+*U*, U_{eff}=7.8 eV.

the orbital potential on the valence- and conduction-band levels are presented in Fig. 4. The bands are indexed *A*, *B*, and *C* from the highest to the lowest energy. It is seen that the band gap increases monotonically with *U*, whereas the *A*-*B* and *A*-*C* separations decrease.

The excitonic spectra calculated with the LDA+*U* band structure (U_{eff}=7.8 eV) is presented in Fig. 5. For the non-SOC calculations the doubly degenerate peak visible for per-

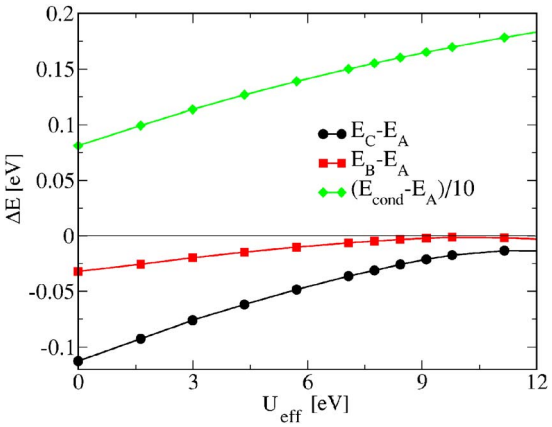

FIG. 4. (Color online) Position of the valence and conduction bands calculated with LDA+*U* as a function of U_{eff}.

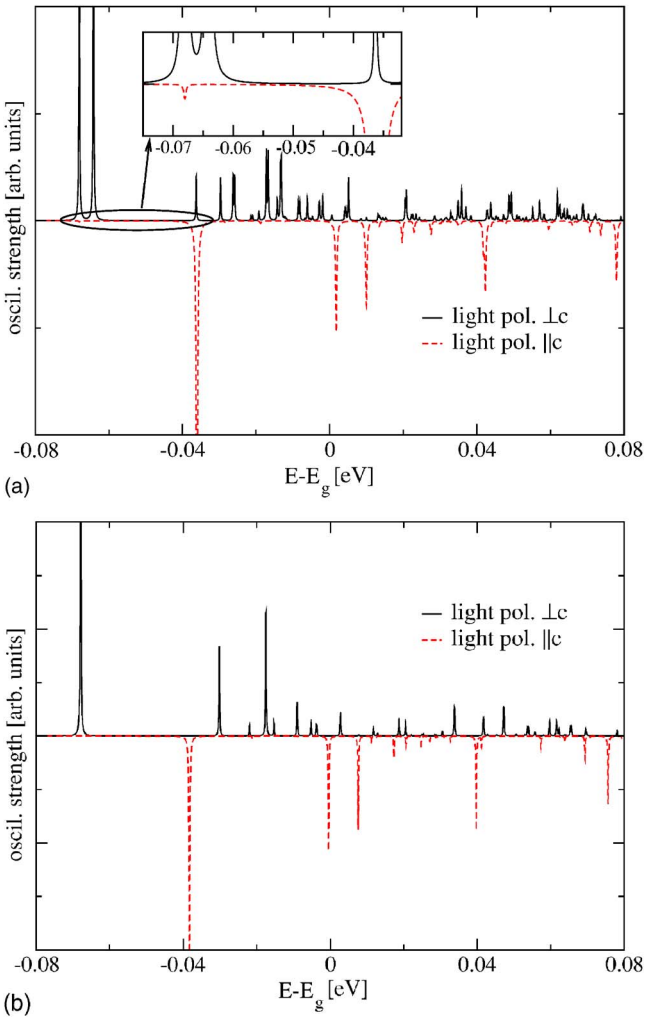

FIG. 5. (Color online) Band-edge absorption in ZnO calculated with LDA+U, (a) results with SOC, (b) results without SOC.

pendicular light polarization is about 68 meV below the conduction-band edge, 10 meV lower than for the $U=0$ case. As an apparent improvement over the pure GGA calculations the peak related to the exciton C is now inside the band gap, about 38 meV below the conduction-band edge (active for polarization parallel to the c axis). For the SOC calculations the splitting of the A and B excitons is now only about 3.5 meV, which is much closer to the experimental value of 2.4 meV than the GGA value of 30 meV. The crystal-field-induced splitting between A-B and C excitons is similar in both SOC and non-SOC cases, and is about 30 meV. The experimental splitting is about 40 meV.[41] Besides these great improvements of the excitonic spectra the symmetry properties of the A and B excitons have not been changed by application of the orbital potential. The inset in Fig. 5(a) shows that the first peak is also visible for light polarized parallel to the c axis, indicating the Γ_7 character of the contributing valence band.

The variational coefficients $A^{\lambda}_{vc\mathbf{k}}$ define the contributions of the elementary excitations between a valence v and a conduction c band at the $\mathbf{k}$ point of the BZ to the excitonic wave function. The analysis shows that at the Γ point of the BZ the

TABLE I. Conduction- and valence-band separation (E_c-E_v) and excitation and binding energies.

SOC	band	E_c-E_v [eV]	Excit. energy [eV]	Bind. energy [meV]
−	A,B	3.3550	3.2873	67.8
−	C	3.3835	3.3168	66.7
+	A	3.3489	3.2809	67.9
+	B	3.3527	3.2848	67.9
+	C	3.3797	3.3129	66.8

A, B, and C excitons originate from the separate levels. For non-SOC calculations they are single states, for the SOC case they are a combination of doubly degenerate levels. It is then convenient to index these bands according to the excitons they contribute. In such a case it is possible to define the binding energy for each exciton as a difference between the energy difference of conduction and valence bands (E_c-E_v) and the excitation energy. In the experimental literature the binding energy is usually determined from the difference between the ground and excited levels of exciton utilizing Elliott's model.[44] Assuming the Elliott model is correct these two ways of calculating the binding energy are equivalent. As the exciton is excited from its ground state it becomes more localized in $\mathbf{k}$ space[34] and its energy level approaches the band energy difference. In principle both ways can be applied for the calculated spectra. However, in the calculation it is very difficult to determine precisely the energy of the excited states due to enormous density of the required $\mathbf{k}$ mesh. Table I collects the energy separation of the conduction and valence bands, excitation energies, and the binding energies for LDA+U calculation with and without SOC. The binding energies for all excitons are comparable, despite the difference in the excitation energies. It is worth noting that non-SOC calculations result in exactly the same binding energies as the calculations with SOC.

The calculated spectra presented in Figs. 2 and 5 show that the excitons A and B are visible mainly in the light polarized perpendicular to the crystallographic c axis, while the C exciton is visible for light polarized parallel to this axis. When the SOC is included the tiny absorption of the exciton A is also observed in the light polarized parallel to the c axis and also exciton C is excited in the perpendicularly polarized light. These effects find an elegant explanation that follows from the already mentioned group theoretical arguments. They can also be understood by analyzing the characters of partial charges (electron numbers) at Zn and O muffin-tin spheres contributed from A-, B- and, C-band levels at the Γ point of the BZ. Such a splitting is presented in Table II. The conduction band is mainly s character. Thus for the optical excitation the p character of the valence bands is the most important. As we see the p character is concentrated on the O atom. For the non-SOC calculations A and B states are pure p_{x+y} while the C state is pure p_z. The photon polarized parallel to the c axis interacts with p_z orbitals and the polarized perpendicularly interacts with only p_{x+y}. The effect of the SOC is that some of the p_z characters appear in the A state and p_{x+y} in the C state. Thus in this case A and C excitons can be excited by light in both polarizations.

TABLE II. Partial charges at the Γ point.

SOC	band	atom	p_z	p_{x+y}	d_{z^2}	$d_{x^2-y^2}+d_{xy}$	$d_{xz}+d_{yz}$
−	A,B	Zn	0.0	0.01	0.0	0.2	0.09
−	A,B	O	0.0	0.60	0.0	0.0	0.0
−	C	Zn	0.0084	0.0	0.26	0.0	0.0
−	C	O	0.62	0.0	0.0	0.0	0.0
+	A	Zn	0.0	0.01	0.0	0.109	0.042
+	A	O	0.0013	0.703	0.0	0.0	0.0
+	B	Zn	0.0	0.010	0.0	0.101	0.045
+	B	O	0.0	0.705	0.0	0.0	0.0
+	C	Zn	0.0087	0.0	0.129	0.0	0.0
+	C	O	0.714	0.0011	0.0	0.0	0.0

Calculation of the optical absorption in a wide range of photon energies requires an approach, which is different from the one described above. First, a complete sampling of the full BZ has to be applied. Fortunately, a much lower **k**-point density can be used in this case, as we are not interested in the very fine details of the absorption edge. Second, a much larger range of excitation energies needs to be considered, implying that more conduction and valence bands have to be included in the BSE Hamiltonian. The resulting dimension of the BSE Hamiltonian is much larger than for the calculations of the binding energies. In our case, $15\times15\times9$ **k**-point mesh, with six valence and eight conduction bands, the size of the Hamiltonian is almost 10^5. Diagonalization of such a large matrix would be impractical. Instead, we use the so-called "time evolution" algorithm introduced by Schmidt *et al.*[45] where $\varepsilon_2(\omega)$ is evaluated without explicitly calculating excitonic eigenvalues and eigenvectors. Figure 6 shows the calculated $\varepsilon_2(\omega)$ with both DFT (without electron-hole interaction) and BSE. As expected,[34] the electron-hole interaction enhances the spectra in the low-energy region (up to 8 eV) and reduces the absorption for larger energies. However, the main features are recognized in both cases. For instance, for perpendicular polarization two peaks are well visible in both the DFT (9 eV and 13 eV) and BSE (8 eV and 11 eV) curves.

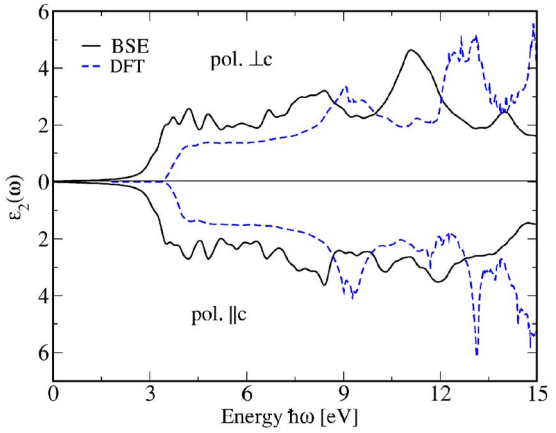

FIG. 6. (Color online) Imaginary part of the dielectric function, $\varepsilon_2(\omega)$, calculated within the BSE formalism (solid line) and the DFT with scissor shift (dashed line) for two polarizations with respect to the c direction of the hexagonal unit cell (perpendicular and parallel in the upper and lower panels, respectively). In both cases the band structure was calculated with orbital field (LDA+U). A broadening of 0.2 eV was used to generate the BSE curves.

IV. SUMMARY AND CONCLUSIONS

The present *ab initio* calculations of the band-edge optical absorption in ZnO include the effects of electron-hole correlations as accounted for by solving the Bethe-Salpeter equation. The band structure was determined in the framework of DFT, however with a band gap, which has been corrected by means of a scissors operator. Three excitons indexed as A, B, and C have been identified. It has been shown that, due to too-high-lying Zn 3d states, standard DFT-GGA calculations result in spectra with the wrong A-B splitting and the C exciton located in the conduction band instead in the band-gap region. These problems were solved by applying the LDA+U scheme with parameters, which have been extrapolated from the linear dependence determined for the series of 3d metals, from Ti to Cu, in $LaMO_3$.[19] The LDA+U calculations not only improve the calculated optical response but also result in a DOS with the correct energy position of the Zn 3d peak. This shows that the linear dependence is more general and applicable at least to the Zn case. The calculated binding energies of the A, B, and C excitons are similar and equal to 68–67 meV. The binding energy of the C exciton is only 1 meV smaller than the A and B excitons. This is close to the experimentally determined range of 60–50 meV.[40,41] The calculations without SOC showed that the photons polarized perpendicular to the crystallographic c axis interact with excitons A and B only, whereas the C exciton is visible only for parallel polarization. The SOC effects in splitting the degenerate A and B excitons and makes the A visible also in the parallel polarization. For the C exciton SOC makes it visible in the perpendicular-polarized light. These effects are related to the SOC introduced admixture of p_{x+y} character in the C band, and p_z in the A band. This also shows that according to our results the A band is of Γ_7 symmetry.

ACKNOWLEDGMENTS

We are grateful to the "EXCITING" European Research and Training Network for providing financial support (Con-

tract No. HPRN-CT-2002-00317). N.E.C. acknowledges support from the Danish Natural Science Research Council, Grant No. 21-03-0340. The calculations were performed at the Center for Scientific Computing in Aarhus (CSCAA), financed by the Danish Center for Scientific Computing (DCSC) and the Faculty of Science, University of Aarhus. We are grateful to N.C. Hansen, system manager at CSCAA, for excellent advice in connection with our heavy computing tasks. We also would like to thank G. K. H. Madsen for fruitful discussions.

[1] T. Miyata, T. Minami, K. Sakai, and S. Takata, J. Lumin. **60**, 926 (1994).
[2] S. Nakamura, T. Mukai, and M. Senoh, Appl. Phys. Lett. **64**, 1687 (1994).
[3] D. M. Bagnall, Y. F. Chen, Z. Zhu, T. Yao, S. Koyama, M. Y. Shen, and T. Goto, Appl. Phys. Lett. **70**, 2230 (1997).
[4] C. Weisbuch, M. Nishioka, A. Ishikawa, and Y. Arakawa, Phys. Rev. Lett. **69**, 3314 (1992).
[5] M. Zamfirescu, A. Kavokin, B. Gil, G. Malpuech, and M. Kaliteevski, Phys. Rev. B **65**, 161205(R) (2002).
[6] L. C. LewYan Voon, M. Willatzen, M. Cardona, and N. E. Christensen, Phys. Rev. B **53**, 10703 (1996).
[7] D. G. Thomas, J. Phys. Chem. Solids **15**, 86 (1960).
[8] J. J. Hopfield, J. Phys. Chem. Solids **15**, 97 (1960).
[9] Y. C. Park, C. W. Litton, T. C. Collins, and D. C. Reynolds, Phys. Rev. **143**, 512 (1966).
[10] D. C. Reynolds, D. C. Look, B. Jagai, C. W. Litton, T. C. Collins, T. Harris, M. J. Callahan, and J. S. Bailey, J. Appl. Phys. **86**, 5598 (1999).
[11] S. F. Chichibu *et al.*, Semicond. Sci. Technol. **20**, S67 (2005).
[12] S. Adachi, K. Hazu, T. Sota, S. ChiChibu, G. Cantwell, D. C. Reynolds, and C. W. Litton, Phys. Status Solidi C **2**, 890 (2005).
[13] A. V. Rodina, M. Strassburg, M. Dworzak, U. Haboeck, A. Hoffmann, A. Zeuner, H. R. Alves, D. M. Hofmann, and B. K. Meyer, Phys. Rev. B **69**, 125206 (2004).
[14] B. K. Meyer, H. Alves, D. M. Hofmann, W. Kriegseis, D. Foster, F. Bertram, J. Christen, A. Hoffmann, M. Strassburg, M. Dworzak, U. Haboeck, and A. V. Rodina, Phys. Status Solidi B **241**, 231 (2004).
[15] W. R. L. Lambrecht, A. V. Rodina, S. Limpijumnong, B. Segall, and B. K. Meyer, Phys. Rev. B **65**, 075207 (2002).
[16] N. E. Christensen, *High Pressure in Semiconductor Physics I*, edited by T. Suski and W. Paul, Vol. 54 of *Semiconductors and Semimetals*, edited by R. K. Willardson and E. R. Weber (Academic Press, New York, 1998), p. 49.
[17] N. E. Christensen and M. Methfessel, Phys. Rev. B **48**, 5797 (1993).
[18] A. Svane, Phys. Rev. B **53**, 4275 (1996).
[19] I. Solovyev, N. Hamada, and K. Terakura, Phys. Rev. B **53**, 7158 (1996).
[20] S. Albrecht, L. Reining, R. Del Sole, and G. Onida, Phys. Rev. Lett. **80**, 4510 (1998).
[21] L. X. Benedict, E. L. Shirley, and R. B. Bohn, Phys. Rev. Lett. **80**, 4514 (1998).
[22] M. Rohlfing and S. G. Louie, Phys. Rev. Lett. **81**, 2312 (1998).
[23] G. Strinati, Phys. Rev. Lett. **49**, 1519 (1982).
[24] G. Strinati, Phys. Rev. B **29**, 5718 (1984).
[25] S. L. Adler, Phys. Rev. **126**, 413 (1962).
[26] N. Wiser, Phys. Rev. **129**, 62 (1963).
[27] M. S. Hybertsen and S. G. Louie, Phys. Rev. B **34**, 5390 (1986).
[28] J. F. Muth, J. H. Lee, I. K. Shmagin, R. M. Kolbas, H. C. Casey, B. P. Keller, U. K. Mishira, and S. P. Den Baars, Appl. Phys. Lett. **71**, 2572 (1997).
[29] P. Blaha, K. Schwarz, G. K. H. Madsen, D. Kvasnicka, and J. Luitz, computer code WIEN2K, an augmented plane wave plus local orbitals program for calculating crystal properties. Vienna University of Technology, Austria, 2001.
[30] G. K. H. Madsen, P. Blaha, K. Schwarz, E. Sjöstedt, and L. Nordström, Phys. Rev. B **64**, 195134 (2001).
[31] P. Puschnig and C. Ambrosch-Draxl, Phys. Rev. B **66**, 165105 (2002).
[32] P. Puschnig and C. Ambrosch-Draxl, Phys. Rev. Lett. **89**, 056405 (2002).
[33] K. Hummer, P. Puschnig, and C. Ambrosch-Draxl, Phys. Rev. Lett. **92**, 147402 (2004).
[34] R. Laskowski, N. E. Christensen, G. Santi, and C. Ambrosch-Draxl, Phys. Rev. B **72**, 035204 (2005).
[35] J. P. Perdew, K. Burke, and M. Ernzerhof, Phys. Rev. Lett. **77**, 3865 (1996).
[36] V. I. Anisimov, J. Zaanen, and O. K. Andersen, Phys. Rev. B **44**, 943 (1991).
[37] V. I. Anisimov, I. V. Solovyev, M. A. Korotin, M. T. Czyżyk, and G. A. Sawatzky, Phys. Rev. B **48**, 16929 (1993).
[38] M. T. Czyżyk and G. A. Sawatzky, Phys. Rev. B **49**, 14211 (1994).
[39] A. G. Petukhov, I. I. Mazin, L. Chioncel, and A. I. Lichtenstein, Phys. Rev. B **67**, 153106 (2003).
[40] K. Hümmer, Phys. Status Solidi **56**, 249 (1973).
[41] A. Mang, K. Reimann, and S. Rübenacke, Solid State Commun. **94**, 251 (1995).
[42] R. T. Girard, G. C. Tjernberg, S. Söderholm, U. O. Karson, C. Wigren, H. Nylén, and I. Lindau, Surf. Sci. **373**, 409 (1997).
[43] G. K. H. Madsen, Europhys. Lett. **373**, 409 (2005).
[44] R. J. Elliott, Phys. Rev. **108**, 1384 (1957).
[45] W. G. Schmidt, S. Glutsch, P. H. Hahn, and F. Bechstedt, Phys. Rev. B **67**, 085307 (2003).